Mechanics and Mechanical Engineering
Vol. 14, No. 2 (2010) 233–246

Post–Critical Deformation State of a Multi–Segment Multi–Member Thin–Shell Structure Subject to Torsional Deflection

Tomasz Kopecki
Department of Aircraft and Aircraft Engines
Rzeszów University of Technology
W. Pola 2, 35–959 Rzeszów, Poland

Hubert Dębski
Department of Mechanical Engineering
Lublin University of Technology
Nadbystrzycka 36, 20–618 Lublin, Poland

Received (18 June 2010)
Revised (18 July 2010)
Accepted (23 July 2010)

A three–segment ten–member thin–shell structure with flat walls is considered made of material with instantaneous characteristic approximated by means of an ideally elastic–plastic material model. The structure material (polycarbonate) demonstrates the temporary double refraction effect in polarized light. The system is subject to twisting resulting in state of local post–critical deformation of skin segments within the structure area that is interpreted, in first approximation, as a field of drawing forces. As a result of non–linear numerical analysis in the course of which conformance of equilibrium paths obtained numerically and by means of the experiment is assured, the stress field is determined taking into account the structure's flexural and membrane state.

Keywords: Shell, finite elements, nonlinear analysis, experiment, buckling, post–critical state

1. Introduction

Thin–shell load–bearing systems of aviation structures are characterized by admissibility of certain local loss of skin elements stability in conditions of operational loads [1, 10]. That results from the fact that the commonly adopted static model of a structure composed of a framing and a skin represents a semi–monocoque structure in which it is assumed that function of the skin consists in transfer of static interactions only. The framing, composed of transversally situated ribs (frames) characterized with large stiffness in their planes and members demonstrating large stiffness for normal forces and relatively small stiffness for bending, is a mechanism.

Joined with the skin, the framing creates a structure able to transfer any loads resulting from any potentially arising admissible flight phases.

As for transfer of loads by individual structure elements, the cases in which twisting is the dominant form of load generating the pure shear state in isolated skin elements between neighboring frames and members turn out to be the dimensioning ones for the skin elements. These elements, when subject to shearing, loose quickly their stability at relatively low critical compressive stress values. An important stage in design work on an aircraft load–bearing structure with significant effect on relation between its mass, stiffness and load capacity limit, consists in choice of number of frames and members resulting in level of internal load exerted on skin elements in post–critical deformation conditions [7].

This paper presents a conception concerning analysis of a multi–segment semi–shell structure subject to dominant twisting resulting in local post–critical deformation state in skin elements based on an example case of 3–segment 10–member structure. The structure was subject to nonlinear numerical analysis in the finite element approach verified by means of experimental work. Results of experimental research created the possibility to perform corrections of the numerical model in such a way that, at any stage of the structure's deformation advancement, conformance of equilibrium paths and deformation form was assured. Conformance of these results constituted a base for acknowledgement that the structure's stress patterns obtained by means of nonlinear numerical analysis are reliable.

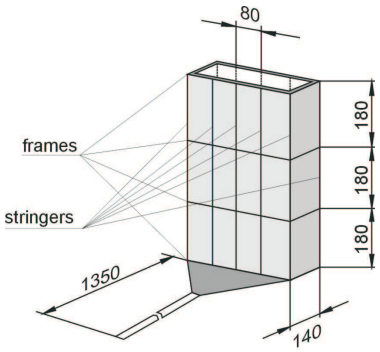

Figure 1 Schematic view of the structure (dimensions in millimeters)

2. Subject and scope of research

The subject of research consisted in a three–segment thin–shell structure with ten members, general view of which is presented in Fig. 1. Joints between the structure elements were realized by means of densely distributed bolts (pitch $t = 15$ mm).

Experimental research was carried out by mounting the structure on specially designed test stand (Fig. 4) making possible to introduce a load in the form of dominant twisting with negligible bending effect and transversal force. One of the structure's boundary frames was fixed, while the other was connected, by means

of a stiff rib closing the cross-section, with a lever by means of which the load was applied gravitationally. Schematic view of the mounting and introduction of load to the structure is presented in Fig. 2.

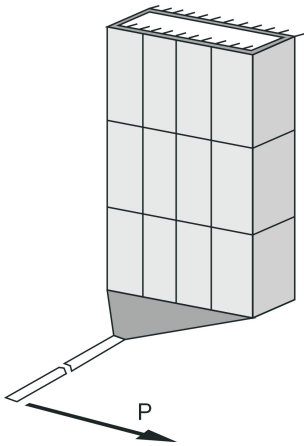

Figure 2 Schematic view of structure mounting and load application

The structure was made of polycarbonate — a material with instantaneous characteristic presented in Fig. 3.

The permanent deformations range resulting from change of the polymer molecules position and shape corresponds in its nature to the plastic range of an elastic–plastic material. That enabled to approximate the actual characteristic with an ideally elastic–plastic material model in the course of numerical analysis. Moreover, polycarbonate demonstrates the temporary double refraction effect. Observation of optical effects in circularly polarized light creates a possibility to obtain a qualitative information about existence and location of strong stress concentration zones, especially in advanced deformation states [8, 9]. In order to enable observation of the above-mentioned effects, inner surface of skin elements were coated with a reflexive layer. Observations was carried out using the reflected light method.

In the course of experiment the load was increased gradually, at very small increment values, with model torsion angle being measured accordingly. As a result, dependence between the twisting moment and the structure's total torsion angle was obtained, i.e. the parameters determining representative equilibrium path of the system (Fig. 9).

Already at relatively small values of twisting moment, all skin segments reached the post–critical deformation state. After full release of load, the structure returned to its initial form. Therefore, despite significant post–critical deformations, permanent deformations did not occur in the advances deformation phase. In Fig. 5, advanced phase of deformation of the model is presented. Fig. 6 shows the corresponding patterns of optical effects.

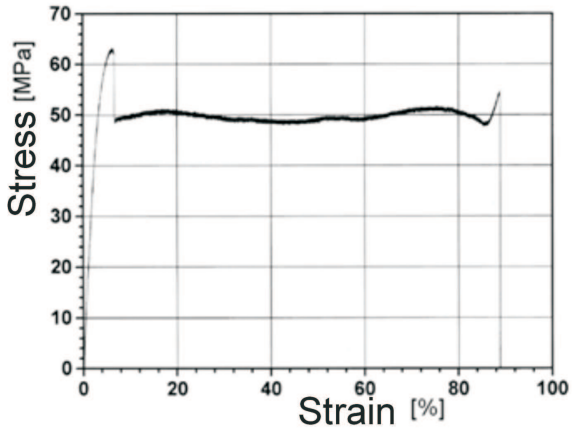

Figure 3 Structure material (polycarbonate) tensile graph

Figure 4 View of the test stand

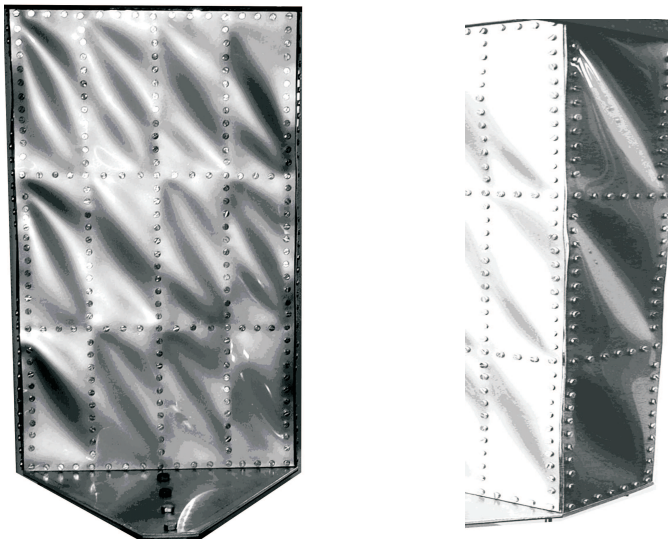

Figure 5 Advanced phase of deformation of the structure

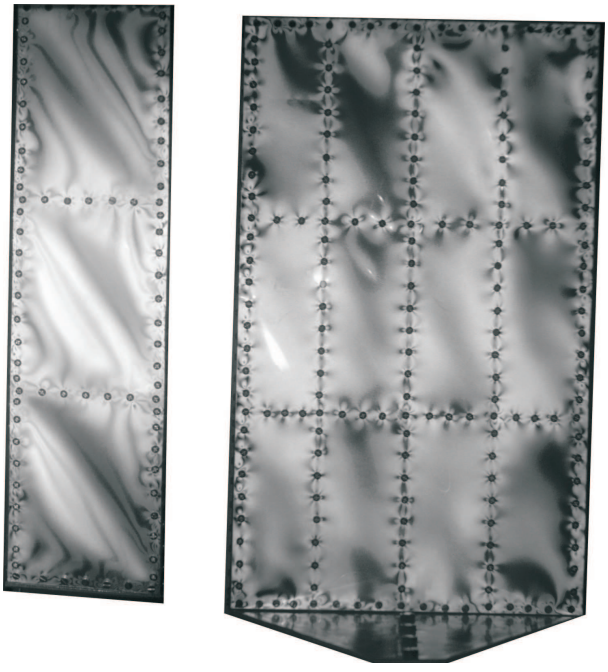

Figure 6 Optical effect patterns

The obtained representative equilibrium path and the observed optical effect patterns created a base for assessment of results obtained by means of nonlinear numerical analyses.

3. Nonlinear numerical analysis

In nonlinear analysis of load–bearing structures, relations between a set of static parameters and the corresponding set of geometric parameters can be presented in the form of matrix equation:

$$\mathbf{g} = \mathrm{K}^{-1}(\mathbf{g})\mathrm{f} \tag{1}$$

where **g** is a set of geometric parameters describing the system deformation state caused by the load, f is a set of static parameters, while K is the stiffness matrix depending on the set of geometric parameters determining current deformation state and a nonlinear constitutive relation.

In view of occurrence of permanent deformations observed in the course of experiments, the structure material's physical characteristic determined in the uniaxial tensile stress tests (Fig. 3) was approximated by an ideally elastic–plastic body model (Fig. 7).

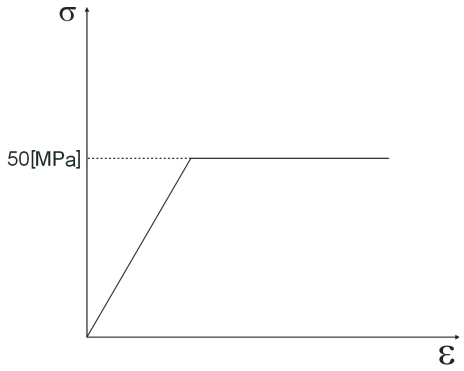

Figure 7 The material's constitutive model

In the constitutive equation, in description related to the linear-elastic range,

$$\sigma = \mathbf{D}\varepsilon \tag{2}$$

assumption about invariance of normal segment ($\varepsilon_z = 0$) was kept in force. Therefore the plate stress state is represented by vector $\sigma = \{\sigma_x, \sigma_y, \tau_{xy}, \tau_{yz}, \tau_{zx}\}^T$, while

$$\mathbf{D} = \frac{E}{1-\nu^2}\begin{bmatrix} 1 & \nu & 0 & 0 & 0 \\ \nu & 1 & 0 & 0 & 0 \\ 0 & 0 & \frac{1-\nu}{2} & 0 & 0 \\ 0 & 0 & 0 & \frac{1-\nu}{2k} & 0 \\ 0 & 0 & 0 & 0 & \frac{1-\nu}{2k} \end{bmatrix} \tag{3}$$

is the material constants matrix in which effect of non–dilatational strain on the plate elastic energy was accounted for by introducing a correction coefficient $k = 1.2$;

$$\varepsilon = \left\{ \varepsilon_x,\, \varepsilon_y,\, \frac{1}{2}\gamma_{xy},\, \frac{1}{2}\gamma_{yz},\, \frac{1}{2}\gamma_{zx} \right\}^T$$
$$= \left\{ \begin{array}{l} \frac{\partial u}{\partial x} + \frac{1}{2}\left[\left(\frac{\partial u}{\partial x}\right)^2 + \left(\frac{\partial v}{\partial x}\right)^2 + \left(\frac{\partial w}{\partial x}\right)^2 \right] \\ \frac{\partial v}{\partial y} + \frac{1}{2}\left[\left(\frac{\partial u}{\partial y}\right)^2 + \left(\frac{\partial v}{\partial y}\right)^2 + \left(\frac{\partial w}{\partial y}\right)^2 \right] \\ \frac{\partial u}{\partial y} + \frac{\partial v}{\partial x} + \left(\frac{\partial u}{\partial x}\right)\left(\frac{\partial u}{\partial y}\right) + \left(\frac{\partial v}{\partial x}\right)\left(\frac{\partial v}{\partial y}\right) + \left(\frac{\partial w}{\partial x}\right)\left(\frac{\partial w}{\partial y}\right) \\ \frac{\partial u}{\partial z} + \frac{\partial w}{\partial y} + \left(\frac{\partial u}{\partial y}\right)\left(\frac{\partial u}{\partial z}\right) + \left(\frac{\partial v}{\partial y}\right)\left(\frac{\partial v}{\partial z}\right) + \left(\frac{\partial w}{\partial y}\right)\left(\frac{\partial w}{\partial z}\right) \\ \frac{\partial u}{\partial z} + \frac{\partial w}{\partial x} + \left(\frac{\partial u}{\partial x}\right)\left(\frac{\partial u}{\partial z}\right) + \left(\frac{\partial v}{\partial x}\right)\left(\frac{\partial v}{\partial z}\right) + \left(\frac{\partial w}{\partial x}\right)\left(\frac{\partial w}{\partial z}\right) \end{array} \right\} \tag{4}$$

is a vector containing deformation state components corresponding to the Green–Saint–Venant deformation tensor [11]; and u, v, w are displacement vector components in local system of coordinates x, y, z.

Numerical representations of the system's nonlinear deformations are based on assumption that, at any solution stage with the corresponding load, the deformed system retains always a static equilibrium state. Thus, for a defined discrete system it is possible to formulate a system of equilibrium equations that, with respect to nonlinear structural analysis in its displacement–based representation, can be expressed in the form of matrix equation for residual forces,

$$\mathbf{r}(\mathbf{u},\, \Lambda) = 0 \tag{5}$$

where $\mathbf{u}$ is the state vector containing structure nodes' displacement components corresponding to current geometrical configuration, Λ is a matrix composed of control parameters corresponding to current load state, while $\mathbf{r}$ is the residual vector containing uncompensated components of forces related to current system deformation state [5, 6].

In numerical algorithms, components of matrix Λ are expressed as functions of parameter λ described as the state control parameter. It is a measure of increase of load related indirectly or directly with the pseudo–time parameter t. Thus, the system of equilibrium equations (5) can be also presented in the form:

$$\mathbf{r}(\mathbf{u},\, \lambda) = 0 \tag{6}$$

The above equation is known as the monoparametric equation of residual forces. Its solution includes a finite number of consecutive structure deformation states, where each state corresponds to a combination of varying control parameters related to the system load, expressed by a single state control parameter λ. Transition from current state to the consecutive one, representing the increment step, is initialized by a change of the control parameter, to which a new structure geometry is related determined by a new state vector.

Development of numerical methods reflected in contemporary algorithms implemented in professional commercial programs resulted in constitution of their two fundamental types. The first one includes purely incremental methods known

also as prediction methods, while the other type encompasses correction methods, called also prediction–correction or increment–iteration methods. The first of the mentioned groups is characterized with limited, often unsatisfactory accuracy of obtained results. Moreover, they do not provide possibility to continue calculations after crossing critical points on the equilibrium path. Introduction of the iteration phase is therefore aimed at reduction of solution error and possibility to determine critical points. That makes possible to analyze a structure in advanced deformation states.

A feature common for both method types consists in presence of the incremental phase. With respect to arbitrary increment, at transition from n–th to $(n\,+\,1)$–th state, the undetermined quantities are:

$$\Delta\mathbf{u}_n = \mathbf{u}_{n+1} - \mathbf{u}_n \qquad \text{and} \qquad \Delta\lambda_n = \lambda_{n+1} - \lambda_n \tag{7}$$

In order to determine them, an additional increment control equation is formulated, known as the equation of constraints, expressed in the form of condition:

$$c(\Delta\mathbf{u}_n,\, \Delta\lambda_n) = 0 \tag{8}$$

The fundamental component of the increment phase consists in its prediction step, determining a point in state hyperspace corresponding to the consecutive state configuration, defined by determination of increment $\Delta\mathbf{u}$ for assumed $\Delta\lambda$, with equation (8) satisfied as the same time. Error of the solution at each increment step depends on the increment control equation and the adopted extrapolation formula. In each consecutive increment step, value of total error may increase, resulting in occurrence of the so–called drift error. Its minimization is ensured by the iteration phase.

The fundamental method used in solution of structural mechanics nonlinear problems is the Newton–Raphson method with numerous program realizations and variations constituting a family of methods [4, 5, 6, 7]. The core idea of these methods consists in expansion of the residual forces equation, $\mathbf{r} = \mathbf{0}$, and the increment control equation, c = 0, into Fourier series.

Assuming that, as a result of k–th correction iteration step, values $\mathbf{u}^k$ and λ^k are obtained, the equations will take the following forms:

$$\mathbf{r}^{k+1} = \mathbf{r}^k + \frac{\partial\mathbf{r}}{\partial\mathbf{u}} \cdot \mathbf{d} + \frac{\partial\mathbf{r}}{\partial\lambda} \cdot \eta + H = \mathbf{0} \tag{9}$$

$$c^{k+1} = c^k + \frac{\partial c}{\partial\mathbf{u}} \cdot \mathbf{d} + \frac{\partial c}{\partial\lambda} \cdot \eta + H = 0 \tag{10}$$

where:

$$\mathbf{d} = \mathbf{u}^{k+1} - \mathbf{u}^k \qquad \eta = \lambda^{k+1} - \lambda^k \tag{11}$$

Terms H in both equations include neglected residual values of higher orders. In the iteration process, consecutive values of $\mathbf{d}$ and η are determined with respect to which the solution convergence condition is checked at assumed tolerance. The set obtained that way, constituting a solution of nonlinear algebraic equations with respect to unknown nodal displacements, creates a base for determination of equilibrium path. The path, representing a relation between static parameters corresponding to the structure and geometrical parameters related to displacements of

its individual points represents a hyper–surface in a multidimensional space with number of dimensions corresponding to number of degrees of freedom of the system taken into account. In practice, representative relations between two parameters are usually developed.

In order to obtain an additional method that could be used to verify results obtained with and compare capabilities of two independent software types, the numerical analysis was carried out by means of ABAQUS/STANDARD 6.8-3 and MSC MARC 2007 programs. In case of ABAQUS software package, two versions of numerical model were developed. In both versions, Shell S4–type elements were used for skin modeling, while members were represented by Beam 2.1–type elements. The difference between the models consisted in different representation of frames. In the first version's model, a three-dimensional representation was applied with the use of Solid C3D8–type elements, with a total of 7895 nodes obtained. In the second version, Shell S4-type elements were used as a result of which a total of 16779 nodes were obtained.

On the other hand, when using MSC MARC 7 software, thin–shell type bilinear elements were used to model the examined structure's skin, while thick–shell type elements were applied for modeling frames and the load application system. Members were represented by beam-type elements based on the Euler–Bernoulli method. All the above–mentioned elements have six degrees of freedom per node, thus full conformity between skin elements and members was secured. A total of 25300 nodes was obtained.

Nonlinear analysis carried out by means of ABAQUS package revealed an excessive quantitative divergence between obtained numerical results and the experiment in case of frames being represented by three–dimensional elements, therefore that type of solution was abandoned in case of MARC program.

The non-linear analysis was based on the Newton–Raphson prediction method [2, 3, 4, 5, 6, 12] and the Crisfield hyperspherical correction. Reliability of the obtained results was assessed by comparing both equilibrium path shapes and deformation geometries. The two elements created a base for repeated corrections of numerical model.

As a result of a series of numerical tests, models were developed in which nature of deformation corresponded fully and qualitatively to deformations obtained in the course of experiment. For all model versions, likewise in the course of experimental research, dependence was being determined between the overall torsion angle and the twisting moment value, constituting representative equilibrium paths.

Fig. 8 presents the structure's geometrical model obtained by means of MSC PATRAN software and the finite element grid adopted for calculations with the MSC MARC program.

Comparison of representative equilibrium paths is presented in Fig. 9.

In Figs. 10 and 11, the reduced stress distributions according to H–M–H hypothesis are presented for all model versions, corresponding to the advanced deformation phase.

Comparison of equilibrium paths and deformation type allows to acknowledge the nonlinear numerical analysis results as satisfactory ones. It should be also emphasized that refinement of numerical models was possible only in view of possibility to compare results of calculations with those obtained in the experiment. Even min-

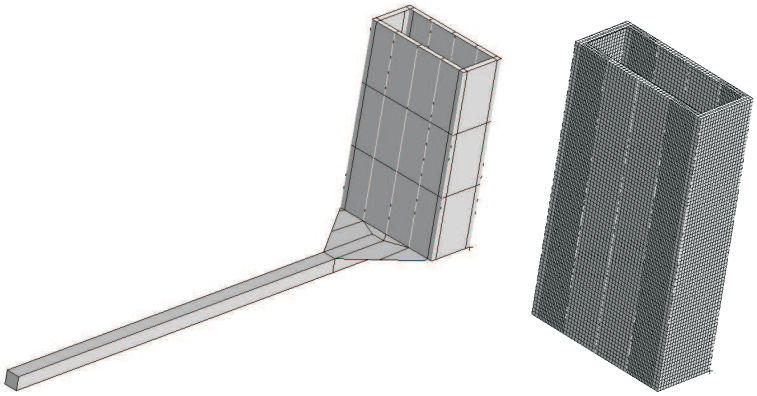

Figure 8 Geometrical model (left) and the finite element grid (right)

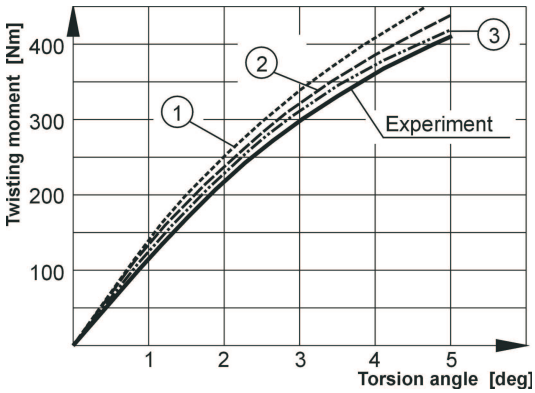

Figure 9 Comparison of representative equilibrium paths: 1 – Calculations performed with ABAQUS program – frames modeled with three–dimensional elements; 2 – Calculations performed with ABAQUS – frames modeled with shell elements; 3 – Calculations performed with MSC MARC program

imal corrections to stiffness of structure elements can result in fundamental changes in the equilibrium path course or lack of the numerical solution's convergence. Furthermore, on the grounds of the solution uniqueness rule providing that a specific deformation form can correspond to one and only one stress distribution, the effective stress distributions determined numerically can be acknowledged as corresponding to actual ones. An additional qualitative criterion of verification of calculation results consists in comparison of obtained effective stress distribution patterns with optical effect images observed in the course of experiments.

Development of a numerical model that can be accepted as a satisfactory one creates a possibility to make changes in the structure's design solution in a virtual environment aimed at representation of possible special geometrical features such

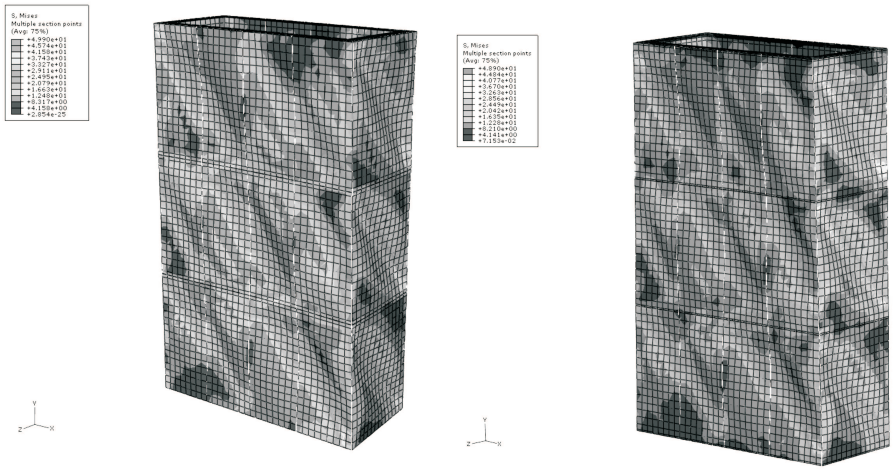

Figure 10 Results of calculations performed with ABAQUS STANDARD program: The numerical model deformation picture and the effective stress distribution according to Huber–Mises–Hencky hypothesis. (a) — model with two-dimensional frames; (b) — model with three-dimensional frames

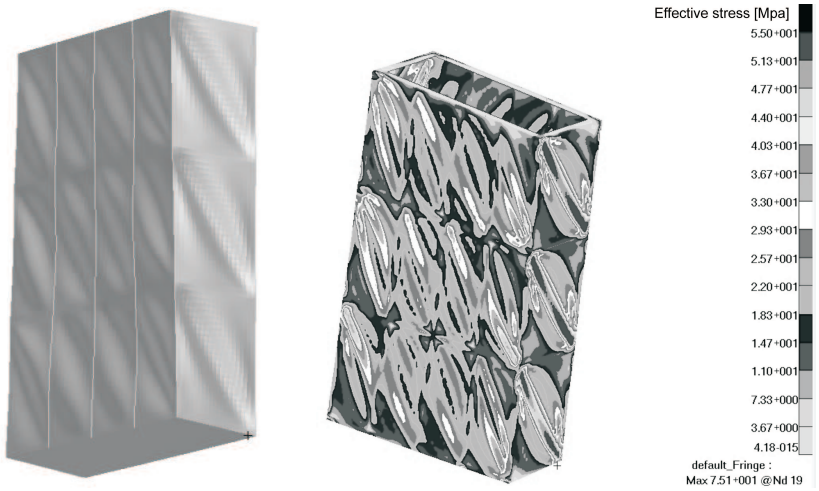

Figure 11 Results of calculations performed with MSC MARC 7 program: The numerical model deformation picture and the effective stress distribution according to H–M–H hypothesis

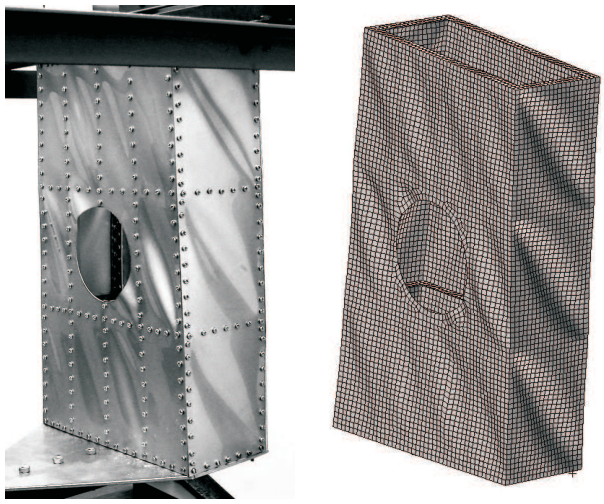

Figure 12 Advanced phase of post–critical deformations for a model with circular opening: result of the experiment (left) and that of nonlinear numerical analysis

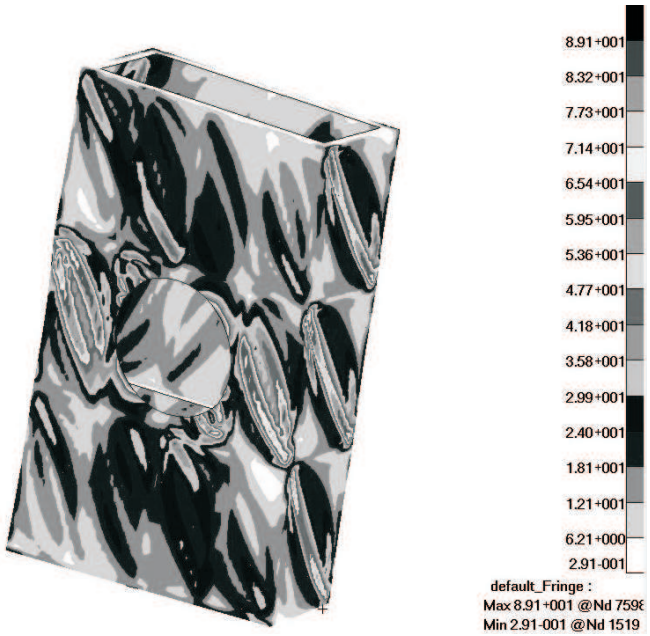

Figure 13 The effective stress distribution according to Huber–Mises–Hencky hypothesis for a model with circular opening

as e.g. defects or cut–outs. In case of the analyzed structure, one of the structure's wall was subject to modification consisting in introduction of representation of a circular cut–out (Fig. 12). Nonlinear analysis was carried out with the use of identical numerical methods and iteration parameters.

Using the test set–up described above, an experiment was carried out with the use of model provided with a circular opening. Fig. 12 presents comparison of the structure's post–critical deformation pictures obtained from the model experiment on one hand and nonlinear numerical analysis on the other.

The presented results confirm full relevance of the deformation form. Comparison of total distortion angle values for selected twisting values also allows to note that there exists a satisfactory quantitative conformance between results of calculations and experiments. Therefore, the effective strain pattern presented in Fig. 13 can be considered a reliable one.

4. Conclusions

The presented method of determination of effective stress distributions in a thin–shell structure working in the post–critical load range based on verification of results obtained from numerical analyses by means of the experiment, allows to localize effectively any stress concentration zones and carry out appropriate modifications of the structure. Such modifications can be performed in the virtual environment created by MES software, making possible to choose properly the number and the geometry of frames and members as well as eliminate other imperfections of the structure. That makes possible to refine the structure's design before fabrication of its prototype, representing usually one of the most expensive stages in the process of development of a new construction design.

It should be underlined that elimination of structure imperfections by means of combination of nonlinear numerical analysis with the experiment and analysis of numerical models subject to modifications can be applied at relatively early design process stage.

The numerical model providing conformance with the experiment and the adopted problem solving strategy create a base for numerical analysis of a series of the structure's modified geometry variants without necessity to repeat the experimental component of research, thus eliminating possible irrational solutions through implementation of the prototype design.

References

[1] **Arborcz, J.**: Post–buckling behavior of structures, Numerical techniques for more complicated structures, *Lecture Notes In Physics*, 228, **1985**.

[2] **Bathe, K.J.**: Finite element procedures, *Prentice Hall*, **1996**.

[3] **Doyle, J.F.**: Nonlinear analysis of thin–walled structures, *Springer–Verlag*, New York, Berlin, Heidelberg, **2001**.

[4] **Crisfield, M.A.**: Non–linear finite element analysis of solid and structures, *J. Wiley & Sons*, New York, **1997**.

[5] **Felippa, C.A., Crivelli, L. A. and Haugen, B.**: A survey of the core–congruential formulation for nonlinear finite element, *Arch. of Comput. Meth. in Enging.*, 1, **1994**.

[6] **Felippa, C.A.**: Procedures for computer analysis of large nonlinear structural system in large engineering systems, ed. by A. Wexler, *Pergamon Press*, London, **1976**.

[7] **Kopecki, T. and Dębski H.**: Buckling and post–buckling study of open section cylindrical shells subjected to constrained torsion, *Arch. of Mech. Enging.*, Vol. LIV, 4, **2007**.

[8] **Kopecki, H.**: Problemy analizy stanów naprężenia ustrojów nośnych, w świetle badań eksperymentalnych metodami mechaniki modelowej, *Zeszyty Naukowe Politechniki Rzeszowskiej*, Nr 78, Rzeszów, **1991**.

[9] **Laerman, K.H.**: The principle of integrated photo-elasticity applied to experimental analysis of plates with nonlinear deformation, Proc. 7^{th} Conf. on experimental stress analysis, Haifa, **1982**.

[10] **Lynch, C.**: A finite element study of the post buckling state behaviour of a typical aircraft fuselage panel, PhD. Thesis, *Queen's University*, Belfast, **2000**.

[11] **Marcinowski, J.**: Nieliniowa stateczność powłok sprężystych, *Oficyna Wydawnicza Politechniki Wrocławskiej*, Wrocław, **1999**.

[12] **Rakowski, G. and Kacprzyk, Z.**: Metoda elementów skończonych w mechanice konstrukcji, *Oficyna Wydawnicza Politechniki Warszawskiej*, Warszawa, **1993**.